INTERNATIONAL ATOMIC ENERGY AGENCY
UNITED NATIONS EDUCATIONAL, SCIENTIFIC AND CULTURAL ORGANIZATION
INTERNATIONAL CENTRE FOR THEORETICAL PHYSICS
I.C.T.P., P.O. BOX 586, 34100 TRIESTE, ITALY, CABLE CENTRATOM TRIESTE

H4.SMR/383 - 25

WORKSHOP ON REMOTE SENSING TECHNIQUES WITH APPLICATIONS TO AGRICULTURE, WATER AND WEATHER RESOURCES

(27 February - 21 March 1989)

APPLICATIONS OF AN ATMOSPHERIC BOUNDARY LAYER MODEL

ALBERTO L. FLORES
Universidad de Buenos Aires
Departamento de Meteorologia
Pabellon II, 2 do Piso
Buenos Aires 1428
ARGENTINA

APPLICATIONS OF AN ATMOSPHERIC BOUNDARY LAYER MODEL

Alberto L. Flores
Workshop on Remote Sensing Techniques with applications to Agriculture, Weather and Water Resources
International Centre for Theoretical Physics
February 27 - March 21, 1989.
Trieste, Italy

1.- Introduction

Remote determination of soil moisture and antecedent precipitation is of particular importance in agriculture, hydrology and meteorology. Carlson et al. (1984) and Carlson (1985) show that a useful parameter for describing the soil water deficit is the moisture availability (M), defined as the ratio of evaporation to potential evaporation. Introduced by Manabe (1969) for use in climate modelling, the moisture availability has been adapted by Carlson et al (1981) and others (Price, 1982; Wetzel et al, 1984; Taconet et al, 1986) as the essential surface parameter that governs the partition between sensible and latent heat flux at the surface. Surface temperature during summertime conditions of large radiational forcing is very sensitive to surface moisture, at least when the soil is moderately dry.

Shukla and Mintz (1982)show that the global fields of rainfall, temperature and motion strongly depend on the land-surface evapotranspiration. In that way they confirm that the surface vegetation, which produces the evapotranspiration, is an important factor in the earth's climate. Using a one-dimensional boundary layer model, one can solve for the moisture availability by inverting the simulated surface temperatures with the remote measurements of surface temperature. Although the method has both its advantages and disadvantages, preliminary analyses indicate that it is sufficiently sensitive to resolve the total range of soil dryness between absolutely dry and field saturation into about 4 or 5 subranges of dryness (Carlson, 1985). It is not possible to verify the remotely determined soil moisture (M) fields from a satellite, but a convenient indicator of the ground wetness is the antecedent precipitation. In conditions of subsaturation in the soil, runoff is relatively small and the stored soil moisture is closely related to the antecedent precipitation. Thus, Wetzel et al (1984) and Carlson et al (1984) were both able to find high correlations over Kansas between antecedent precipitation fields and the moisture availability using GOES data for the temperature measurements. Taconet et al (1986), using simple pixel temperature measurements made aboard the NOAA-7 satellite, found that in the absense of precipitation, the moisture availability over an agricultural region in France decreased to levels equivalent to wilting in the upper layers of the soil. There are also different approximations to the problem, like the SiB model (Sellers et al, 1986). More simple models, mainly aimed to agricultural applications were used by Vidal et al (1987).

In the absence of a current capability for global routine daily soil moisture observation, is convenient to present methods with some capability to fulfill that role. Practical methods applicable to remote sensing of vegetation covered surfaces are limited to two basic wavelenght bands: the thermal infrared and the microwave.Each of these has its special advantages and disadvantages, which often work in a manner that allows the two observations to complement one another. Microwave techniques, which rely on the large effect that water content has on the dielectric constant of soil, have the advantage of a wide dynamic range in the signal between wet and dry soils. They also enable the observer to take measurements through nonprecipitating clouds. On the other hand, the thermal infrared observation of soil moisture has the advantage of requiring a vastly more modest sensing system. Currently, the microwave is not operational, for that reason we have to rely on the thermal infrared for the next 3-4 years.

In this paper the extension of the method developed by Carlson is presented for two additional case studies using GOES, one over Texas and the other over Argentina. Derived moisture availability fields are compared with antecedent precipitation for these two cases. A slight shift in emphasis is made in this paper from that in earlier articles: here we explore the idea that it may be useful to infer recent precipitation over arid regions in which may be few rainfall measurements. In subsequent sections we present some basic definitions relating to the model, outline the procedure for obtaining the moisture availability and then discuss the case studies.

2. The model

The model, a somewhat updated version of that described by

Carlson (1985), is a one-dimensional, initial value, time-dependent boundary layer model. A surface energy balance equation constitutes the fundamental constraint at the surface.

$$R_n = G_o + H_o + L_e E_o = R_s + R_L - R_l \quad (1)$$

Where R_n is the net radiation, G_o the sensible heat into the ground, H_o the sensible heat into the atmosphere and $L_e E_o$ the latent heat flux. They are compensated by R_s, the short wave radiation; R_L, the backscattered longwave radiation and R_l, the longwave radiation. Flux equations for heat, water vapor and momentum govern the surface layer in the atmosphere.The sensible heat is expressed as:

$$H_o = \frac{\rho C_p (T_o - T_a)}{R_h + R_{ch}} \quad (2)$$

where ρ is dry air density, C_p, the specific heat, T_o and T_a are the temperatures at the soil-air interfase and at some a level above the surface, respectively. R_h and R_{ch} are resistances for atmospheric flux, through a surface and through a ground/air transition layer, respectively.

Profiles of temperature are calculated in the soil by means of a force-restore method similar to that described by Deardorff (1978):

$$G_o = \frac{\lambda (T_o - T_{-1})}{\Delta Z_o} \quad (3)$$

being λ the thermal conductivity of the soil, T_o , the temperature at interfase level, and T_{-1} the temperature at the first level into the ground. ΔZ_o is the corresponding depth.

The change of temperature in the ground was carried out through the diffussion equation:

$$\frac{\delta T}{\delta t} = \kappa \frac{\delta^2 T}{\delta Z^2} \quad (4)$$

κ is the thermal diffusivity of the subtrate.

Thermal inertia (P), the governing substrate parameter for the diffusive heat flux, is calculated from the model and defined as follows,

$$P = (\lambda\kappa)^{-1/2} \tag{5}$$

The latent heat flux, L_eE_o is expressed as:

$$L_eE_o = \frac{\rho L_e M(q_o(T_o) - q_a)}{R_v + R_{cv}} \tag{6}$$

Being M, the moisture availability, q_o the specific humidity, that refers to the level at the ground surface, where the air is saturated at surface temperature T_o, and at a reference level (z_a) where q equals q_a. R_v and R_{cv} are resistances for the atmospheric flux, respectively, through a surface and through a ground/air transition layer. These resistances are calculated internally from conventional similarity equations. They are calculated for sensible and latent heat in a similar way:

$$R_h + R_{ch} = \int_0^{z_a} \frac{dz}{K_h(z) + C_h/\rho C_p} \tag{7}$$

replacing the subindexes conveniently.In this equation $K_h(z)$ is the eddy transfer coefficient, C_h is a molecular diffussion coefficient.

M is a conceptual quantity (Carlson, 1985), defined by the equation:

$$M = \frac{R_v + R_{cv}}{R_v + R_{cv} + R_c} = \frac{E_o}{E_o(T_o)} \tag{8}$$

where R_c is the bulk canopy (soil and vegetation) resistance and $E_o(T_o)$ is the "potential" evaporation from the canopy. Although M is slightly dependent on the choice of the reference height for computing R_v, it is a slowly varying parameter during the day and fundamentally related to soil moisture content in the upper root zone of the soil W_g. Therefore, we let $M = \frac{W_g}{W_{fs}}$, where W_{fs} is the field saturation water content. R_c or M constitute the basic unknown, which is determined by inversion of the model using the measured radiometric surface temperatures.

Once performed the inversion of the model, M fields are compared with antecedent precipitation, which is essentially a running

mean rainfall amount. An antecedent precipitation index (API) has been defined by Saxton and Lenz (1967), Choudhury et al (1983) and used by Carlson et al (1984) in comparing fields of M with antecedent precipitation.

The API is here defined as:

$$API_i = kAPI_{i-1} + R_i \tag{9}$$

where the subscripts refer to day i or i-1. R_i is the rainfall on day i and k is a weighting coefficient; an optimum value for k, which is that used in this study, is 0,92. (Wetzel and Woodward, 1987). API is initialized using the mean monthly precipitation at some time prior to the period of interest. Since the value is roughly equivalent to a three-week mean precipitation amount, the contribution by initial API becomes insignificant afer several weeks.

3. The method and the data

Moisture availability and thermal inertia are the primary governing parameters in the model. It is possible to determine these two parameters uniquely, given measured surface temperatures near midday and the other during the nighttime or predawn hours, provided that other parameters in the model are specified. Carlson and Boland (1978) show that the two most sensitive parameters in the model are M and P and that the remaining parameters such as wind speed or albedo can be either calculated internally or specified with sufficient accuracy to permit a unique solution for these two parameters. Wetzel et al (1984) show that M itself is most sensitive to the rate of increase of temperature during the morning. Both Wetzel et al and Carlson et al (1984) apply the method using morning temperature rises to infer moisture availability. Thermal inertia, however, is not obtainable because it is insensitive to the rate of temperature rise during the morning.

Accordingly, M was calculated to the changes of temperature between early and late morning (ΔT_o) GOES satellite images. Given two temperature images provided by a satellite, M was found by transforming the temperature difference fields using algorithms derived from the model results. The algorithms are obtained from model output extracted for the exact times of satellite overpass. Normally, 14 executions of the model are required to produce a complete mapping of T_o to M, given a set of initial model conditions. Initial conditions are furnished from local observations, the nearest atmosphere sounding and from an approximate knowledge of surface roughness and albedo. A climatological mean is used for the initial substrate reservoir temperature.

Infrared imagery supplied by the National Oceanographic and Atmospheric Administration (NOAA) for the SMS/GOES satellite (resolution 8 km) was used to obtain surface temperatures for the two target areas. Atmospheric water vapor corrections were made using a model developed by Price (1983). For the two case studies reported here, the two morning images are near 1200 UTC (about two hours after local sunrise) and 1700 UTC, which is not far from solar noon. Images were extracted for 128 x 128 pixel regions and resampled to know map coordinates.

4.- Case studies

a) Texas and Oklahoma: July, 1980

The location of the target area is shown in Fig. 1. The region is about 300.000 km^2 and includes parts of Texas and Oklahoma. It is divided into two sections, referred to here as the eastern and western, each corresponding to a resampled GOES subset image. The terrain is flat and is covered by unirrigated range and cropland. Altogether three days were examined, July 1, 14 and 29. The period was chosen because it was one of extreme drought over the Great Plains of the United States and, consequently, the terrain was characterized by large horizontal gradients of rainfall, mainly from northeast to southwest. We find that patterns of M derived from the infrared method are more reliable when there is a large range of surface moisture.

Fields of M and API were obtained for each of the three days and for both western and eastern sectors. API was initialized on 1 June. In Figs. 2 and 3 fields of API and M are shown for the western region. Clearly, there is a correspondence between M

and API, with higher values of both appearing in the southwest corner and lower values to the west. Table 1 contains correlations between M and API for each day and region. These results were obtained by extracting point values of each parameter from a 7 x 7 square grid superimposed on the area. Regressions are listed only for cases where the correlation coefficient exceeds 0.5. When data from all days are combined, the correlation coefficient increases to 0.65, suggesting that the correlation improves as the range of values is expanded.

Correlations between API and M were made on a time basis by comparing differences between paired pixels on two days. These results are summarized in Table 2. Here temporal changes in moisture availability (Δ M) are related to temporal changes in antecedente precipitation (Δ API). Correlations are somewhat better for changes occurring between the 1st and 14th of July than for the latter period; they are also better for the eastern region. In general, correlations are better where there is greater spatial variability of API or M.

Combining both regions and the two time intervals (July 1 - 14 and 14 - 29) yields a composite regression equation:

$$\Delta API(mm) = -2.5 + 16.5\Delta M \qquad (10)$$

with a correlation coefficient of 0.79 and "T-ratios" for slope and ordinate of 17.6 and 4.8, respectively. (T-ratios are considered to be significant if their magnitude exceeds 2.0 for a sample size of 49 elements; details concerning this statistical criterion are found in Davies (1973)).

Mean temporal and spatial variations in the east-west distribution of rainfall and M are illustrated in Fig. 4. Normallly, there is a large gradient of precipitation west to east across Oklahoma and Texas, which can be seen in Fig. 4. In the absence of significant rainfall during the first two weeks of July, the permanent gradient of rainfall (and of M) is shifted toward the east. This shift is reflected in the distribution of M, although the increase of rainfall between the 14th and the 29th east of 97° W seems to have restored the M values over the eastern part of the region to their formerly high values found on July 1st. Further treatment of this case is presented in Flores and Carlson (1985).

b) Argentina

The target area is located over Argentina's central region and extends east-west between 34°S and 39°S and is about 500.000 km^2 (Fig. 5). Analyses were performed for two days, December 24, 1981 and January 18, 1982. Choice of these two days was motivated by three considerations: the season (summer), an absence of cloud and a separation in time less than a month. A further consideration is the large spatial range in precipitation,which varies from about 1000 mm along the coast to about 200 mm at the western end of the hatched area in Fig. 5. Rainfall conditions were quite typical at the times of analysis. The terrain is nearly flat, varying from sea level to about 300 m in the west, and is covered by unirrigated rangeland and cropland.

Infrared imagery was again the SMS/GOES (east) radiometric temperature data at 1200 and 1700 GMT, which are approximately at the same local sun times as the Texas/Oklahoma images discussed above. Daily rainfall data were computed to obtain the API, which was initialized on September 1, 1981. Altogether, there were 71 raingage stations in the area, their locations being indicated by dots in Figs. 6 and 7. M and API fields were analyzed for the two days (not shown) and temporal differences ($\Delta M, \Delta API$) determined by substracting the earlier from the later values. Visual inspection of Figs. 6 and 7 indicate a high correlation between the changes. There is clearly an increase in both parameters over the center of the GOES subset image strip). Correlations were carried out using a 10 x 26 grid overlay for which point values were extracted. The correlation coefficient for the entire region was 0.34 but improved to 0.81 when the subregion was reduced to include only 54 points centered over the region of largest horizontal gradient. In this smaller data set the relationship between ΔM and ΔAPI was found to be:

$$\Delta API(mm) = -15 + 121\Delta M \qquad (11)$$

As in the previous case, the T-ratios were well above the significant level. (11)

5. Conclusions

We have demonstrated that antecedent precipitation and moisture availability derived from infrared surface temperature measurements are correlated on the scale of GOES resolution. The method of determining M appears to be more reliable when there are large horizontal variations in soil moisture and precipitation. A degradation in the correlation occurs with decreasing spatial variation in moisture, a reflection of the inherent uncertainties in the method which seems to possess an intrinsec error corresponding to an uncertainty in moisture availability of plus or minus 15 %. Accordingly, in regions where M varies by much less than its full range (0 to 1.0), the errors may exceed its spatial variation. The weakness in the method does not appear to be fundamentally related to model parameterization or even to the neglect of a specific treatment of vegetation layer in these analyses. Rather it is the complex nature of the surface, the relative insensivity of surface temperature to soil moisture in wet conditions and errors in the measurement itself that impede progress in obtaining reliable soil moisture fields from satellites.

Our results do open an interesting possibility, that of using satellite infrared temperature measurements to infer patterns of recent precipitation. In view of the uncertainties of the method, the technique may be more confidently applied to arid than wet regions. Since rainfall and soil moisture are most critical in such climates, the method may prove to be of value in identifying the onset of drought or in locating recent episodes of rainfall that may be otherwise have occurred unnoticed over the desert.

References

- Carlson, T. N. and F. E. Boland, 1978: Analysis of urban-rural canopy using a surface heat-flux/temperature model, J. Appl.

Meteor., 17, 998-1013.

- Carlson, T. N., J. K. Dodd, S. G. Benjamin and J. N. Cooper, 1981: Remote estimation of surface energy balance, moisture availability and thermal inertia. J. Appl.; Meteor., 20, 67-87, 1981.

- Carlson, T. N., 1985: Regional-Scale Estimates of Surface Moisture Availbility and Thermal Inertia using Remote Thermal Measurements. Remote Sensing Reviews, 1, 197-247, 1985.

- Carlson, T. N., F. G. Rose and E. M. Perry, 1984: Regional-Scale Estimates of Surface Moisture Availability from GOES Infrared Satellite Measurements. Agron. Journal, 76, 972-979.

- Choudhury, B. J. and B. J. Blanchard, 1983: Simulating soil water recession coefficients for agricultural watersheds. Water Resour. Bull. 19, 2, 241-246.

- Davies, J. C., 1973: Statistics and data analysis in geology. John Wiley & Sons, New York, New York.

- Deardorff, J. W., 1978: Efficient prediction of ground surface temperature and moisture with inclusion of a layer of vegetation, J. Geophys. Res. 83, 1889-1904.

- Flores, A. L. and T. N. Carlson, 1985: Acerca de la estimacion de la disponibilidad de humedad en el suelo a partir de mediciones remotas. Geoacta, 13, 137-146.

- Flores, A. L., 1986: On the estimation of rainfall fields. Proceedings of the 2nd Conference on Satellite/Meteorology Applications. American Meteorological Society. Williamsburg, Va (USA). 12-16 May. pp 512-517.

- Flores, A. L. and T. N. Carlson, 1987: Estimation of surface moisture availability from remote temperature measurements. J. Geophys. Res. 92, *N°* D8, 9581-9585.

- Manabe, S., 1969: Climate and Ocean Circulation, I - The Atmospheric Circulation and the Hydrology of the Earth's Surface. Mon. Wea. Rev., 97, 739-774.

- Price, J. C., 1982: On the use of satellite data to infer surface

fluxes at meteorological scales. J. Appl. Meteor., 21, 1111- 1122.

- Price, J. C., 1983: Estimating surface temperatures from satellite thermal infrared data - a simple formulation for the atmospheric effect. Remote sensing of the environment, 13, 353-361.

- Saxton, K. E. and A. T. Lenz, 1967: Antecedent retention indices predict soil moisture. J. of the Hydraulics Div. Proc. of the Amer. Soc. of Civil Eng., HY4, 223-241, July.

- Sellers, P. J., Y. Mintz, C. Y. Sud and A. Dalcher, 1986: A Simple Biosphere Model (SiB) for use within general circulation models. J. Atm. Sciences, 43, 505-531.

- Shukla, J. and Y. Mintz, 1982: Influence of Land-Surface Evapotranspiration on the Earth's Climate. Science, Vol. 215, pp 1498-1501.

- Taconet, O. R., R. Bernard and D. Vidal-Madjar, 1986: Evapotranspiration over an agricultural region using a surface flux/temperature model based on NOAA-AVHRR data. J. Climate Appl. Meteor., 25, 284-307.

Vidal A., Y. Kerr, J. P. Lagouarde and B. Seguin, 1987: Teledetection et bilan hydrique: utilisation combinée dún modèle agrométéorologique et des données del' IR thermique du satellite NOAA-AVHRR. Agric. and Forest. Meteorol., 39, 155-175.

- Wetzel, P. J., D. Atlas and R. Woodward, 1984: Determining soil moisture from geosynchronous satellite infrared data: a feasibility study, J. Clim. Appl. Meteor., 23, 375-391.

- Wetzel, P. J. and R. Woodward, 1987: Soil moisture estimation using GOES-VISSR InfraredData: A Case Study with a Simple Statistical Method. J. Clim. Appl. Meteor., 26, 107 - 117.

Figure legends

Fig. 1: Target area for Texas/Oklahoma case study. The hatched rectangles show the location of the east and west GOES subset regions referred to in the text.

Fig. 2: Antecedent precipitation index (API) for the western GOES subset in Texas/Oklahoma case for 29 July, 1980. Units in mm x 10.

Fig. 3: Moisture availability (M) for the western GOES subset in Texas/Oklahoma case for 29 July, 1980.

Fig. 4: Antecedent precipitation index (top; mm x 10) and moisture availability (bottom) as a function of longitude across the hatched regions in Fig. 1. Values represent lateral averages from top to bottom of the subregions.

Fig. 5: Target area for Argentina case study. The hatched area consists of four subset images whose areas are outlined in Figs. 6 and 7.

Fig. 6: Isopleths of the change in moisture availability (Δ M) between 24 December 1981 and 18 January 1982 over the Argentina target area. Rectangles show the boundaries of the GOES subset images and dots the location of the ground precipitation measurements.

Fig. 7: Isopleths of the change in antecedent precipitation index (Δ API) between 24 December 1981 and 18 January 1982. Units in mm. Other symbols same as in Fig. 6.

TABLE 1

Date, sector, spatial correlation coefficient (R) and linear relationship for Texas/Oklahoma case study, July 1980. API is expressed in mm.

Day	Sector	R	Linear Relationship
1	eastern	0.76	API = 11.8 + 23.5 M
14	eastern	0.14	
29	eastern	0.71	API = 4.5 + 11.2 M
1	western	0.50	
14	western	0.10	
29	western	0.62	API = 2.0 + 9.4 M

TABLE 2

Same as Table 1 but for temporal changes, expressed as Δ M and Δ API.

Day	Sector	R	Linear Relationship
29 - 14	eastern	0.22	
14 - 1	eastern	0.77	Δ API = 0.708 Δ M
29 - 1	eastern	0.32	
29 - 14	western	0.33	
14 - 1	western	0.58	Δ API = - 0.30 + 0.465 Δ M
29 - 1	wetern	0.33	

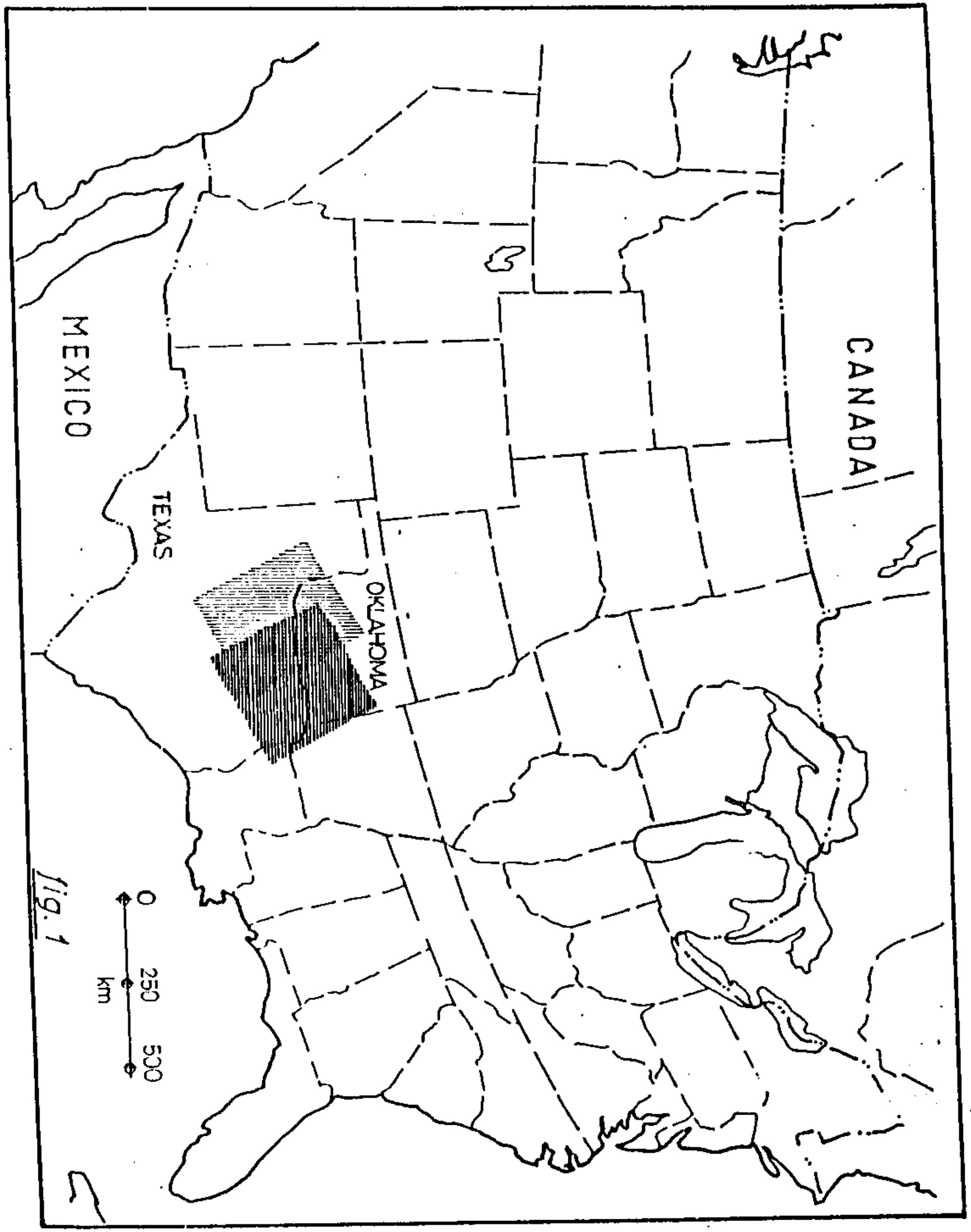

fig. 1

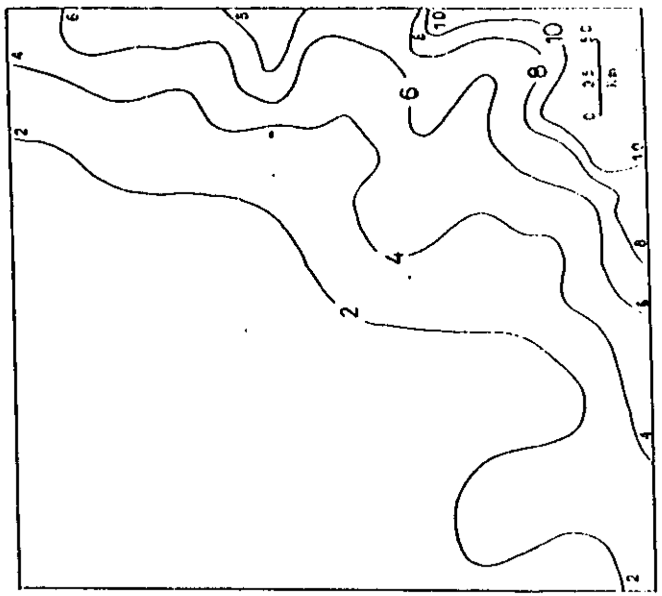

Figure 3. Moisture Availability (x 10) July 29, 1980

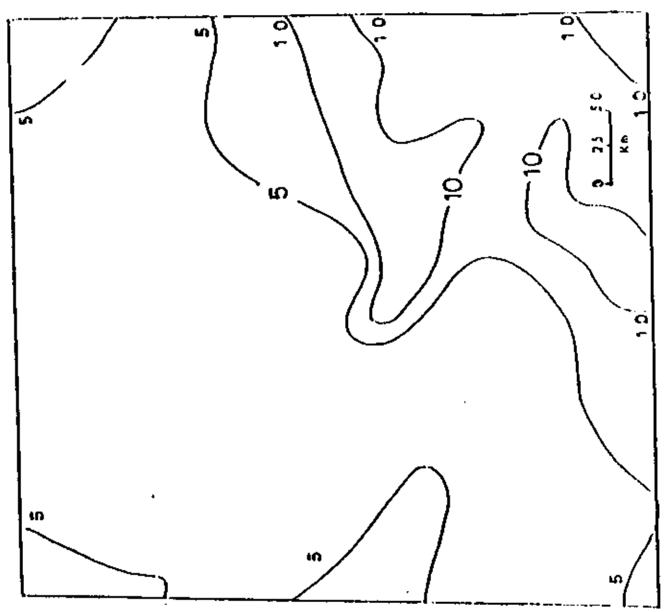

Figure 2 Antecedent Precipitation Index (mm) July 29, 1980

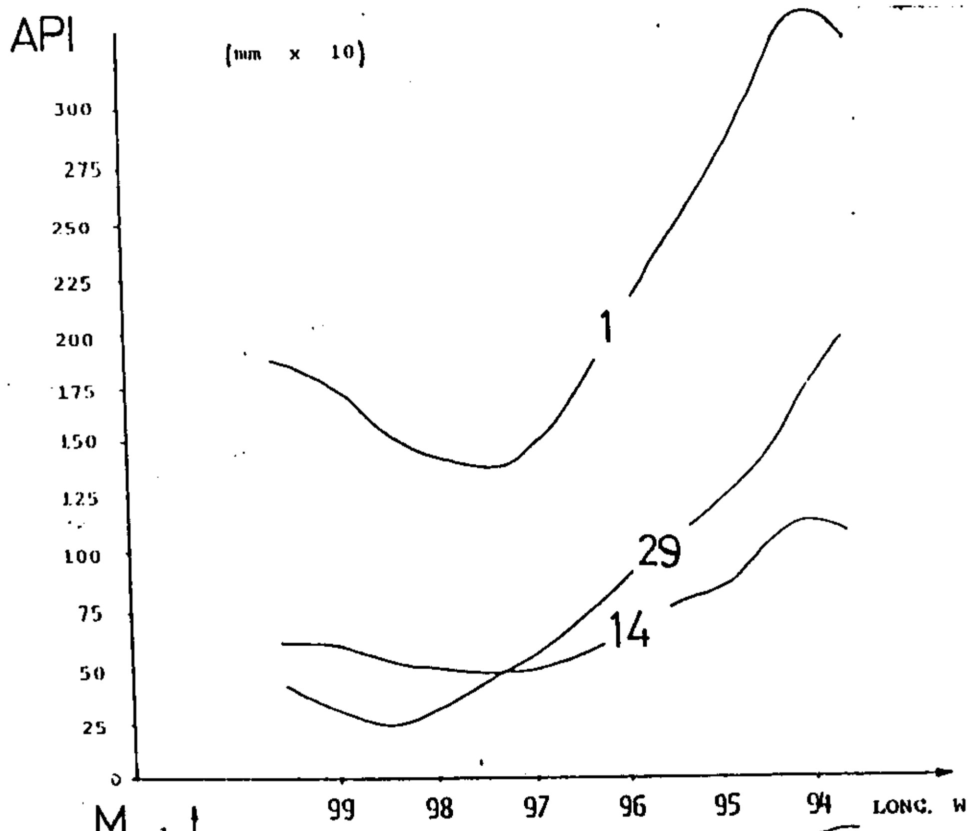

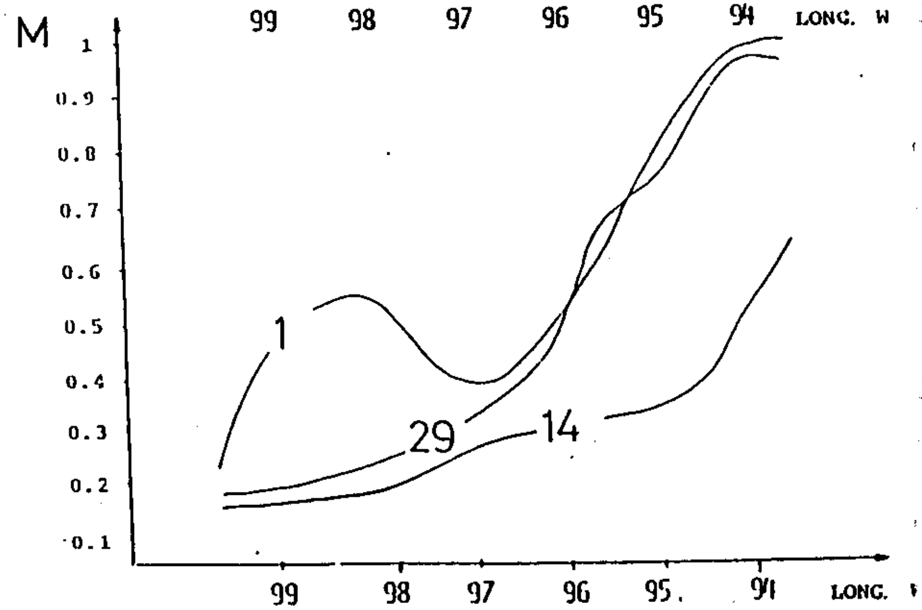

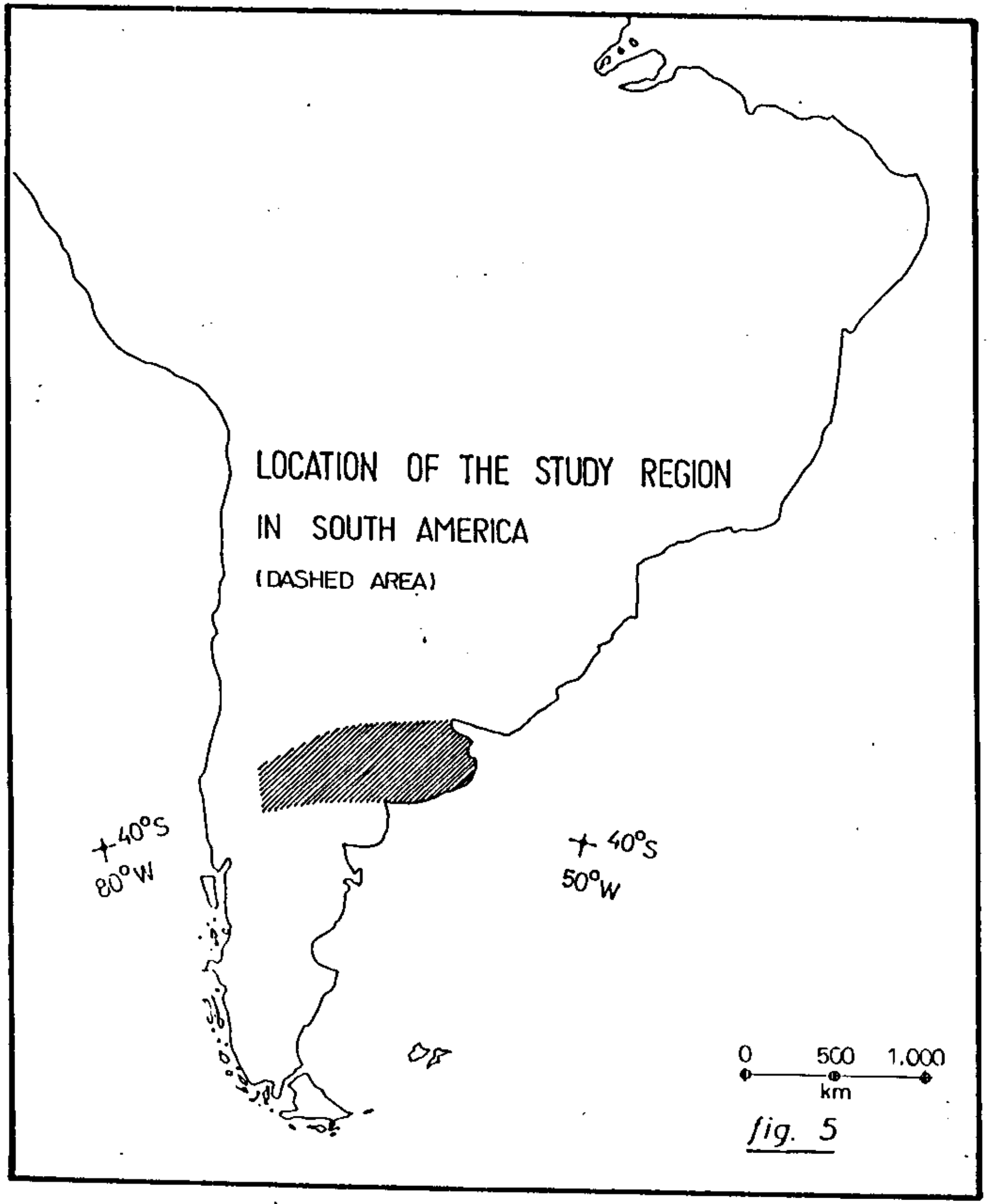

fig. 5

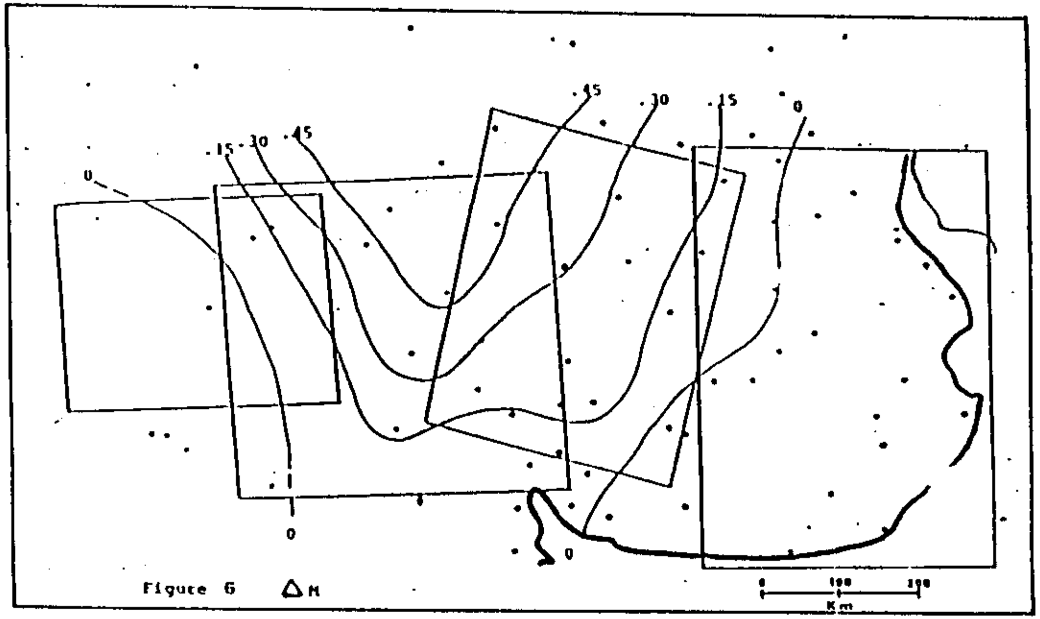

Figure 6 ΔH

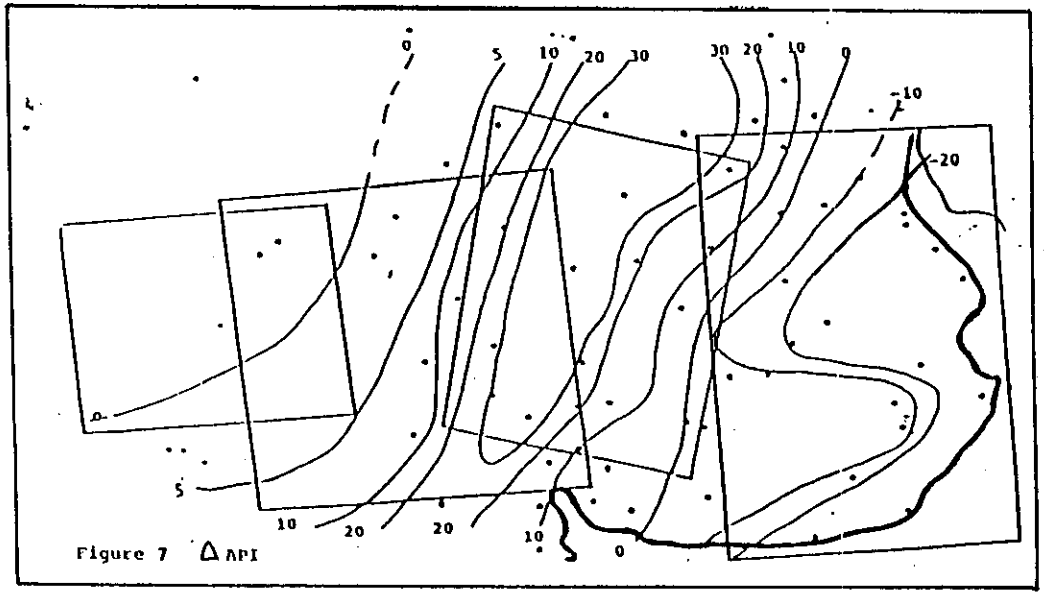

Figure 7 ΔAPI